

JAAS

Accepted Manuscript



This is an *Accepted Manuscript*, which has been through the Royal Society of Chemistry peer review process and has been accepted for publication.

Accepted Manuscripts are published online shortly after acceptance, before technical editing, formatting and proof reading. Using this free service, authors can make their results available to the community, in citable form, before we publish the edited article. We will replace this *Accepted Manuscript* with the edited and formatted *Advance Article* as soon as it is available.

You can find more information about *Accepted Manuscripts* in the [Information for Authors](#).

Please note that technical editing may introduce minor changes to the text and/or graphics, which may alter content. The journal's standard [Terms & Conditions](#) and the [Ethical guidelines](#) still apply. In no event shall the Royal Society of Chemistry be held responsible for any errors or omissions in this *Accepted Manuscript* or any consequences arising from the use of any information it contains.

1
2
3
4
5
6
7
8
9
10
11
12
13
14
15
16
17
18
19
20
21
22
23
24
25
26
27
28
29
30
31
32
33
34
35
36
37
38
39
40
41
42
43
44
45
46
47
48
49
50
51
52
53
54
55
56
57
58
59
60

**A Novel Concentric Grid Nebulizer for
Inductively Coupled Plasma Optical Emission Spectrometry**

Kazumi INAGAKI,^{1*} Shin-ichiro FUJII,¹ Shin-ichi MIYASHITA,¹
Keisuke NAGASAWA,¹ Tetsuya OKAHASHI,¹ Alexander S. GROOMBRIDGE,^{1,2}
Akiko TAKATSU¹ and Koichi CHIBA¹

¹*Environmental Standards Section, National Metrology Institute of Japan (NMIJ),
National Institute of Advanced Industrial Science and Technology, Tsukuba central 3-10,
Umezono 1-1-1, Tsukuba, Ibaraki, 305-8563, Japan.*

²*Nano Doctoral Training Centre, The Cavendish Laboratory, The University of
Cambridge, CB3 0HE, England.*

* To whom correspondence should be addressed.

E-mail: k-inagaki@aist.go.jp, Tel&Fax: +81-29-861-6889

ABSTRACT

1
2
3
4
5
6
7
8
9
10
11
12
13
14
15
16
17
18
19
20
21
22
23
24
25
26
27
28
29
30
31
32
33
34
35
36
37
38
39
40
41
42
43
44
45
46
47
48
49
50
51
52
53
54
55
56
57
58
59
60

A novel concentric type grid nebulizer (CGrid) was developed for sample introduction into inductively coupled plasma optical emission spectrometer (ICP-OES). The CGrid has a concentric structure and a grid screen (over 350 mesh per inch) that is set inside the nozzle. The grid screen acts as both an effective gas-liquid mixing filter and gas flow damper, and then the liquid break-up into small droplets by passing through the grid with a low velocity. By this unique nebulizing process, the CGrid showed excellent nebulizer performances on comparing with commercially available nebulizers such as Meinhard nebulizer type C (MHN), modified high performance concentric nebulizer (m-HPCN), and OneNeb. The primary aerosols generated with the CGrid was finer and their velocity was lower than those with the other nebulizers. This nebulization feature gave a high transport efficiency of aerosol into the plasma, resulting a high sensitivity in ICP-OES. In the range of the liquid flow rate of 0.25 mL min⁻¹ to 2.0 mL min⁻¹ with the optimized nebulizer gas flow rate for obtaining the highest Mg(II)/Mg(I) signal intensity ratio, the maximum loading amount of aerosols into the plasma obtained with the CGrid was higher than those with MHN (2.1-fold) and m-HPCN (1.4-fold), and almost the same as that with OneNeb. The maximum sensitivity in ICP-OES obtained with the CGrid was 1.8- to 3.7-fold, 1.5- to 1.9-fold, and 1.1- to 1.2-fold higher than those with MHN, m-HPCN, and OneNeb, respectively. The CGrid also showed a good tolerance for high total dissolved solid (TDS) concentrations. No clogging was observed when saturated NaCl solution was continuously nebulized for 5 hours. The limit of detections (LODs) obtained with the CGrid were better than those of MHN, 1.6- to 5.3-fold improved, except for Cd I

1
2
3
4 228.802 nm, and almost similar to those of m-HPCN and OneNeb. The plasma
5
6 robustness estimated from the Mg(II)/Mg(I) signal intensity ratio obtained with the
7
8 CGrid (10.6) were also better than those of MHN (9.6), and almost similar to those of
9
10 m-HPCN (10.2) and OneNeb (10.4). The short-term stability on measuring spiked
11
12 seawater (45 min) was within 3 % of relative standard deviation, and the recoveries of
13
14 the spiked elements were in the range of 99 % to 106 %. Validation of the CGrid was
15
16 performed by analyzing the NMIJ CRM 7531-a brown rice flour. The observed values
17
18 for the five elements Mn, Fe, Cu, Zn, and Cd were in good agreement with their
19
20 certified values. It was concluded that the CGrid is very useful for ICP-OES with
21
22 good performance on sensitivity and high TDS solution analysis.
23
24
25
26
27

28 ***Keywords: nebulizer, ICP-OES, aerosol, TDS tolerance.***
29
30
31
32
33
34
35
36
37
38
39
40
41
42
43
44
45
46
47
48
49
50
51
52
53
54
55
56
57
58
59
60

INTRODUCTION

1
2
3
4
5
6
7
8
9
10
11
12
13
14
15
16
17
18
19
20
21
22
23
24
25
26
27
28
29
30
31
32
33
34
35
36
37
38
39
40
41
42
43
44
45
46
47
48
49
50
51
52
53
54
55
56
57
58
59
60

A nebulizer is one of the most important devices in inductively coupled plasma optical emission spectrometry (ICP-OES), as performances such as the nebulization efficiency and tolerance for high total dissolved solid (TDS) concentrations strongly influence the measurement sensitivity and stability in ICP-OES.¹⁻³ A fine nebulization, generating a large amount of fine aerosols (with droplets less than 20 μm in diameter), is beneficial to stability and sensitivity in ICP-OES. Coarser aerosols larger than 20 μm should be cut off by the spray chamber to maintain the stability of the plasma.⁴⁻⁷ Fine aerosols can pass through the spray chamber, so increasing their proportion will increase the amount of aerosol that reaches the plasma, thereby increasing the signal intensity.⁴ A high TDS tolerance is also required as the nebulizer function, because more problematic samples with complicated matrices or high concentrations of salts are routinely analyzed by ICP-OES, especially in material, clinical, biological and environmental research fields.⁸⁻¹²

Several nebulizers have been developed for improving nebulization efficiency and TDS tolerance.³ However, obtaining fine nebulization and a high TDS tolerance are incompatible functions for conventional pneumatic nebulizers, due to their structural limitations. The structure of conventional pneumatic nebulizers are categorized into two types, concentric and non-concentric. In the case of concentric type nebulizers, the nebulization efficiency can be improved by designing a small gas annulus area, but this results in a poor TDS tolerance because salts can easily deposit inside the small gas annulus area. Non-concentric type nebulizers show a high TDS tolerance because clogging by deposition of salts is unlikely to occur due to their structure, but

1
2
3
4 nebulization efficiencies are generally poor due to their smaller gas-liquid contact area.

5
6 More recently, new types of nebulizers that utilize a flow-focusing effect^{13,14} and
7
8 flow-blurring effect^{14,15} have realized fine nebulization along with a high TDS
9
10 tolerance.¹⁶⁻²⁴ We have previously developed a high performance concentric nebulizer
11
12 (HPCN) utilizing the flow-focusing effect.²⁵⁻²⁸ The HPCN has a unique triple-tube
13
14 concentric structure, by which micro-thread liquid flows are formed inside the nebulizer
15
16 nozzle that does not come into contact with the gas exit orifice. These features gives
17
18 both fine aerosol generation and high TDS tolerance. It exhibited high performance
19
20 versus conventional pneumatic nebulizers.^{25,28} However, the structure was a bit
21
22 complicated for large-scale manufacturing.
23
24

25
26 In this work, we newly designed a novel concentric type grid nebulizer (CGrid)
27
28 for ICP-OES instruments. The structure of the CGrid is simple; a grid screen (over
29
30 350 mesh in inch) is only set on the top of a double concentric tube nozzle, of which the
31
32 gas annulus gap between the concentric tubes is larger than that of a conventional
33
34 concentric nebulizer such as Meinhard nebulizer. This structural features gives a
35
36 unique nebulization, which was expected to give not only fine aerosol generation, but
37
38 also a high TDS tolerance. In addition, a manufacturing of the CGrid is easier than
39
40 that of HPCN.
41
42

43
44 Other approaches utilizing grids,²⁹⁻³² such as the Hildebrand nebulizer launched
45
46 by Leeman Lab.,^{31,32} were already presented. The other grid nebulizers require two
47
48 grid screens for improving their nebulization efficiency, due to their parallel path
49
50 structure similar to the V-groove nebulizer,²⁹⁻³² and have a drawback for a memory
51
52 effect in the space between the grids. On the contrary, the CGrid was expected to
53
54 prevent the memory effect, because it required only one grid screen and the space of the
55
56
57
58
59
60

pre-mixing was adequately small for preventing the memory.

In this work, we describe a basic evaluation of the performance of the CGrid, including aerosol diameter and velocity distributions of primary aerosols, TDS tolerance, and analytical performance such as sensitivity, measurement precision, detection limit, and memory effect in ICP-OES, by comparing with three nebulizers such as Meinhard nebulizer as a typical concentric type, modified-HPCN as a flow-focusing type, and OneNeb as a flow-blurring type.

EXPERIMENTAL

Concentric type Grid Nebulizer (CGrid)

A schematic diagram of the CGrid is shown in Fig.1. The CGrid was constructed from a laboratory made PEEK body (nozzle i.d./o.d.: 0.5 mm/6.0 mm, nozzle hole i.d.: 200 μm), PEEK capillary tube (i.d./o.d: 200 μm /400 μm), and PEEK grid screen (356 mesh) set inside the nozzle. The PEEK center capillary was fixed with a 1/16 FEP sleeve and 1/16 PEEK fitting. The tip of the capillary was set at a position recessed by 20-100 μm from the grid screen. The gas back-pressure at an Ar gas flow of 1 L min^{-1} was 60 psi.

Instrumentation

The ICP-OES used was a Perkin-Elmer Optima 7300 DV. The operating conditions were summarized in Table 1. Three types of nebulizers, Meinhard nebulizer type C (MHN: TR-50-C1, Meinhard, US), a modified high performance nebulizer (m-HPCN: AIF-03, S.T. Japan, Japan),²⁸ and OneNeb (Agilent technologies,

1
2
3
4 S/N 10/0218, US), were used for comparing with the performance of the CGrid. All
5
6 the nebulizers were attached to a baffled cyclone spray chamber, and sample solution
7
8 was introduced to the nebulizer using the ICP-OES peristaltic pump. The liquid flow
9
10 rate of sample solution was tested in range of 0.25 mL min⁻¹ to 2.0 mL min⁻¹. In the
11
12 measurements taken, the nebulizer gas flows for each nebulizer were optimized to
13
14 obtain the highest value of the ratio Mg(II) 280.269 nm/Mg(I) 285.213 nm, which is an
15
16 indicator of having robust plasma conditions.³³ The optimized nebulizer gas flow rates
17
18 were in range of 0.55 L min⁻¹ to 0.58 L min⁻¹ for CGrid and OneNeb, and 0.60 L min⁻¹
19
20 to 0.63 L min⁻¹ for MHN and m-HPCN, depending on the liquid flow rates.
21
22

23
24 For evaluating the analytical performance of nebulizers coupled to ICP-OES,
25
26 several atomic and ionic lines covering a wide range of energy sum values (E_{sum} : sum of
27
28 excitation energy (E_{exc}) and ionization energy (E_{ion})) were measured for comparing the
29
30 sensitivity. The emission lines measured were listed in Table 2.
31
32

33 34 35 36 37 **Reagents**

38
39 Working standard solutions in HNO₃ (2 % wt/wt) were prepared from either a
40
41 multielement standard solution containing twenty three elements (ICP Multielement
42
43 standard solution IV CertiPUR, Merck, Damstadt, Germany) or single element standard
44
45 solutions (1000 mg L⁻¹ each, Kanto Chemical Industries, Ltd., Japan). Ultrapure grade
46
47 HNO₃ (Ultrapur[®]100), hydrogen peroxide (Ultrapur[®]) and hydrofluoric acid (Ultrapur[®])
48
49 solutions were purchased from Kanto Chemical, along with analytical grade solid NaCl
50
51 for preparing a saturated NaCl solution (ca. 26 % wt/vol, 20 °C). Pure water prepared
52
53 by a Milli-Q water purification system (resistivity 18 MΩ cm, Nihon Millipore Kogyo,
54
55
56
57
58
59
60

1
2
3
4 Tokyo, Japan) was used throughout the experiments.

5
6 Spiked seawater used for short-term measurement stability and recovery tests was
7
8 prepared by using nearshore seawater certified reference material CASS-4 (National
9
10 Research Council Canada, NRC, CA), where the standard solutions were spiked as 0.5
11
12 mg kg⁻¹ in the sample. Brown rice flour certified reference material NMIJ CRM
13
14 7531-a (National Metrological Institute of Japan, AIST, Japan) was used for the
15
16 analytical validation of the CGrid.
17
18

19 20 21 *Droplet size and velocity measurement*

22
23 The droplet diameter distribution of the primary aerosols was measured by using
24
25 a laser diffraction system (LDS, Aerotrak LDSA-SPR1500A, Nikkiso Co., Japan) at a
26
27 position 5 mm from the nebulizer tip through the centerline of the spray cone. The
28
29 laser focus distance was 100 mm, and the measurement range of the droplet diameter
30
31 (D) was 0.5 μm to 355 μm . Milli-Q water was used as the solution to be nebulized.
32
33 The flow rate of Milli-Q water was set at 1.0 mL min⁻¹ by using a liquid
34
35 chromatography pump (LC-10AD, Shimadzu, Japan). The nebulizer gas was
36
37 controlled with a mass flow control unit (STEC SEC-E400, HORIBA, Japan), and the
38
39 flow rates were set at optimized gas flow rate for obtaining the highest value of the ratio
40
41 Mg(II) 280.269 nm/Mg(I) 285.213 nm in ICP-OES (typically 0.55 L min⁻¹ for CGrid
42
43 and OneNeb, 0.60 L min⁻¹ for MHN and m-HPCN).
44
45
46
47

48
49 The droplet diameter and velocity of the primary aerosols was also measured by
50
51 using a droplet image analyzer (VisiSizer VY system, Oxford lasers, UK) at 10 mm
52
53 from the nebulizer tip through the centerline of the spray cone. The liquid and
54
55 nebulizer gas flow rates were fixed at 1.0 mL min⁻¹ and 0.60 L min⁻¹, respectively, for
56
57
58
59
60

1
2
3
4 evaluating the difference of the velocities.
5
6
7

8 *Estimation of loading amount of aerosols into the plasma*

9

10 The loading amount of aerosols into the plasma was estimated for evaluating the
11 transport efficiency of aerosols into the plasma by using each nebulizer. The system
12 including the nebulizer, spray chamber, and plasma torch injector was constructed
13 outside of the ICP-OES instrument, and a relative volume-concentration of the aerosols
14 passed through the spray chamber and torch injector was measured by the LDS at 3 mm
15 from the tip of the plasma torch injector. The relative volume-concentration was
16 assumed as a relative loading amount of aerosols into the plasma, and was converted to
17 the transport efficiency by calibrating with an absolute loading amount of aerosols by
18 using MHN at the liquid flow rate of 2 mL min⁻¹ measured by a drain collection
19 method,³⁴⁻³⁷ which was almost the same procedure of Gustavsson³⁶ and Pace.³⁷ In
20 brief, prior to collect the drain from the spray chamber, the drain tube and spray
21 chamber was dried by introducing air. Milli-Q water was nebulized, and the drain
22 from the spray chamber was collected for 60 min. The transport efficiency was
23 calculated by subtracting the drain amount from the amount of the introduction liquid
24 into the nebulizer. Milli-Q water was used as the solution to be nebulized. The liquid
25 flow rate tested was in range of 0.25 mL min⁻¹ to 2.0 mL min⁻¹. The nebulizer gas
26 flow rate was set at 0.55 L min⁻¹ for the CGrid and OneNeb, and 0.60 L min⁻¹ for MHN
27 and m-HPCN: those are the almost the same as the optimized gas flow rates.
28
29
30
31
32
33
34
35
36
37
38
39
40
41
42
43
44
45
46
47
48
49
50

51 *Evaluation of Memory effect*

52

53 A wash-in and wash-out performance in ICP-OES was checked for evaluating the
54
55
56
57
58
59
60

1
2
3
4 memory effect, where 2 mL of manganese standard solution of 1 mg L^{-1} was introduced
5
6 at a flow rate of 1 mL min^{-1} by using an inert loop injector (SV-6005N, EYELA, Tokyo,
7
8 Japan), and then the liquid flow-line was washed with 2 % HNO_3 solution. The
9
10 wash-in and wash-out times are referred to the times for obtaining a steady state signal
11
12 from a sample injection and for decreasing the signal to 0.1 % of the steady state signal,
13
14 respectively.
15
16
17
18
19

20 ***Digestion of brown rice flour certified reference material (CRM)***

21
22 The NMIJ CRM 7531-a, brown rice flour, was digested with a microwave
23
24 digestion system (ETHOS 1, Milestone General, Italy). The procedure was the same
25
26 as is described in ref. 28. In brief, approximately 0.5 g of the sub-sample was digested
27
28 with HNO_3 , H_2O_2 and HF. After the digestion, a proper amount of the internal standard
29
30 solution of Y was added into the digest, and then the solution in the vessel was
31
32 evaporated to one drop. Finally, the remaining residue was dissolved in 50 ml of
33
34 0.2 % HNO_3 . A blank solution was also prepared in the same manner.
35
36
37
38
39

40 **RESULTS AND DISCUSSION**

41 ***Characterization of nebulization performance of CGrid***

42
43
44 A nebulizing performance of the CGrid, the droplet diameter and velocity of
45
46 primary aerosols, were characterized on comparing with the other nebulizers.
47
48
49

50
51 The droplet diameter of primary aerosols was measured at a liquid flow rate of 1.0
52
53 mL min^{-1} with two nebulizer gas flow rates; 1.0 L min^{-1} and optimized gas flow rate for
54
55 obtaining the highest value of the ratio Mg(II)/Mg(I) in ICP-OES. The diameters
56
57
58
59
60

1
2
3
4 below which 50 % and 90 % of the aerosol by volume is contained (D_{50} and D_{90}) are
5
6 summarized in Table 3. With both nebulizer gas flow rates, the D_{50} and D_{90} values for
7
8 the CGrid were much smaller than those for MHN. The D_{50} values were also smaller
9
10 than those for m-HPCN and OneNeb, while the D_{90} values are almost the same as those
11
12 for m-HPCN and OneNeb. The diameter distributions patten of primary aerosols at a
13
14 liquid flow rate of 1 mL min^{-1} with optimized gas flow rate, are shown in Fig. 2. All
15
16 of the distributions, except for MHN, are similar patterns, having two peaks around 2
17
18 μm and the other is around $10 \mu\text{m}$, but the first one for the CGrid was *ca.* 1.5-fold
19
20 higher than 40-50 %. These results indicate that the CGrid can generate finer aerosols
21
22 than the other nebulizers.
23
24
25

26
27 Two dimensional distributions of the diameter and velocity of the primary aerosols
28
29 generated with the CGrid and the other nebulizers are shown in Fig. 3, where the liquid
30
31 and nebulizer gas flow rates were fixed at 1.0 mL min^{-1} and 0.60 L min^{-1} , respectively,
32
33 for evaluating the difference of the velocities. The velocities of the primary aerosols
34
35 and their distributions for the CGrid were lower and narrower in a small diameter range,
36
37 respectively, than those for the other nebulizers. In contrast, the distribution of the
38
39 velocities for m-HPCN had a wide distribution, while the droplets were fine. The
40
41 above difference of the fineness and velocity distribution of the primary aerosols was
42
43 mainly due to the difference of the breakup mechanism of liquid into aerosols. In the
44
45 case of MHN, typical pneumatic nebulizer, a small part of the gas kinetic energy is
46
47 transferred to liquid for breaking-up, because only tangential forces of the gas stream
48
49 are acting on the liquid surface, resulting in low nebulization efficiency (efficiency of
50
51 aerosol generation).^{3,14,15} In addition, re-nebulization, which is a major process for
52
53 generating coarse aerosols, occurs at the surface of the nozzle tip.^{3,38} In the case of
54
55
56
57
58
59
60

1
2
3
4 m-HPCN, by flow focusing effect, the re-nebulization does not occur at the nozzle, and
5
6 the nebulizing is focused on the axial-axis.^{25,28} The primary aerosol is much finer than
7
8 that of MHN, while the velocity and their distribution were higher and wider than those
9
10 for the other nebulizers by the focusing effect. In the case of OneNeb, by flow
11
12 blurring effect, gas-liquid premixing occurs inside the nozzle, and the re-nebulization
13
14 also does not occur at the nozzle, while the nebulizing is not focused on the
15
16 axial-axis.^{14,15} Therefore, the primary aerosol is fine and the velocity distribution is
17
18 almost the similar to that of MHN. On the contrary, the nebulizing process of the
19
20 CGrid is different from the other nebulizers, and then the energy transfer in the
21
22 nebulization process was more effective than the other nebulizing process. The grid
23
24 acts as both a gas flow damper and effective gas-liquid mixing filter. Therefore,
25
26 turbulent gas-liquid premixing occurs inside the nozzle by the grid, and then the liquid
27
28 breaks up into small droplets by passing through the grid with low velocity. The
29
30 turbulent premixing would be more effective than the premixing with gas flow blurring
31
32 of OneNeb. In addition, re-nebulization is unlikely to occur because the grid also acts
33
34 as a multi-nozzle reducing re-condensation of the aerosols. In consequence, by the
35
36 unique nebulization mechanism, the CGrid can generate finer and lower velocity
37
38 aerosols than MHN, m-HPCN and OneNeb. This nebulization feature provides a high
39
40 transport efficiency of aerosols into the plasma, as is described in below.
41
42
43
44
45
46
47

48 *Evaluation of transport efficiency of aerosols into the plasma*

49
50 The transport efficiency of aerosols into the plasma with the CGrid was compared
51
52 with those with the other nebulizers, since it directly correspond to the sensitivity in
53
54 ICP-OES. In this comparison, the loading amount of aerosols into the plasma was
55
56
57
58
59
60

1
2
3
4 measured for evaluating the transport efficiency.
5

6 Fig. 4 shows the loading amount of aerosols into the plasma with the CGrid and
7 the other nebulizers in range of a liquid flow rate of 0.25 mL min⁻¹ to 2.0 mL min⁻¹.
8 The loading amount of aerosols with the CGrid saturated at the liquid flow rate of 1.0
9 mL min⁻¹, and the maximum one was higher than those with MHN and m-HPCN, while
10 that by using OneNeb was almost the same level. The transport efficiencies of
11 aerosols were summarized in Table 4. The transport efficiencies with the CGrid were
12 all higher than those with using the other nebulizers in the range of the liquid flow rate
13 of 0.25 mL min⁻¹ to 2.0 mL min⁻¹. The difference in the transport efficiency was
14 owing to differences both of fineness and velocity of the primary aerosols, because the
15 spray chamber acts a momentum (mass and velocity) filter, rather than a size cut-off
16 filter.^{20,39} Smaller aerosols can easily pass through the spray chamber with the
17 nebulizer gas flow, and gravitational and wall-impact losses inside the chamber less
18 occurred. Indeed, the D_{50} values of tertiary aerosols passed through the spray chamber
19 were 3.1 μm for CGrid, 3.8 μm for MHN, 3.7 μm for m-HPCN, and 3.3 μm for OneNeb.
20 In addition, low velocity can be beneficial for reducing aerosol coagulation and
21 wall-impact loss, though a gravitational effect would become large. Therefore, a large
22 amount of aerosols can pass through the spray chamber when the CGrid was used.
23
24
25
26
27
28
29
30
31
32
33
34
35
36
37
38
39
40
41
42
43
44
45

46 *Evaluation of TDS tolerance*

47

48 For evaluating the TDS tolerance of the CGrid, saturated NaCl solution was
49 continuously nebulized at a liquid flow rate of 1.0 mL min⁻¹ with a nebulizer gas flow
50 rate of 0.55 L min⁻¹ for 5 hours, without any washing. Fig. 5 shows microscope photo
51 images of the grid screen before and after nebulizing of saturated NaCl solution. No
52
53
54
55
56
57
58
59
60

1
2
3
4 clogging was observed on the grid, though a few deposition of NaCl on the corner of the
5
6 grid. The diameter distributions of primary aerosols before and after the tolerance test
7
8 were measured for checking the aerosol generation performance. There was little
9
10 change before and after the tolerance test, the D_{50} value measured after the tolerance test
11
12 was $4.0 \mu\text{m} \pm 0.1 \mu\text{m}$ ($n = 10$). In the case of the CGrid, the gas annulus gap ($50 \mu\text{m}$)
13
14 and the size of the holes ($35 \mu\text{m} \times 35 \mu\text{m}$) are both larger than the gap in the gas annulus
15
16 area of conventional pneumatic nebulizers (the gas annulus gaps of MHN and m-HPCN
17
18 are less than $15 \mu\text{m}$). Therefore, clogging by deposition of salts would be unlikely to
19
20 occur inside the nozzle, including the holes of the grid. Taking into account the
21
22 life-time of a plasma torch, 20 % wt/vol salt solution is most likely the maximum level
23
24 of TDS routinely introduced to an axial-view ICP-OES instrument, therefore the CGrid
25
26 has exhibited sufficient TDS tolerance for use in ICP-OES.
27
28
29
30
31
32

33 ***Figures of merit of CGrid in ICP-OES***

34
35 The figures of merit of the CGrid in ICP-OES, such as sensitivity, limit of
36
37 detection, memory effect, and short-term stability of the measurement for the spiked
38
39 seawater, were evaluated by comparing with the other nebulizers. Sensitivity is the net
40
41 intensity of a signal divided by the concentration of analyte.¹ Limit of detection is
42
43 calculated from 3σ of the blank signal ($n = 10$). In this evaluation, the gas flow rate of
44
45 each nebulizer was optimized for each liquid flow rate to obtain the highest value of the
46
47 ratio Mg(II) 280.269 nm/Mg(I) 285.213 nm.
48
49
50
51
52

53 ***Sensitivity***

54
55 The sensitivity of the ion line of Mn (Mn(II) 257.610 nm) in ICP-OES obtained
56
57
58
59
60

1
2
3
4 with the CGrid and the other nebulizers in range of a liquid flow rate of 0.25 mL min⁻¹
5
6 to 2.0 mL min⁻¹, was summarized in Fig. 6, where the sensitivity was shown as the
7
8 relative value for that obtained with MHN at the liquid flow rate of 2.0 mL min⁻¹. As
9
10 is seen in the figure, the trend of the sensitivity is almost similar to that of the transport
11
12 efficiency, except for OneNeb. The maximum sensitivity by using the CGrid was
13
14 about 2.5-fold and 1.7-fold higher than those with MHN and m-HPCN, respectively,
15
16 reflecting the differences in the individual transport efficiencies. On the other hand,
17
18 the maximum sensitivity with the CGrid was also 1.2-fold higher than that with OneNeb,
19
20 in spite of the transport efficiencies with the CGrid and OneNeb were almost the same
21
22 level. This would be mainly attributed to a difference in the fineness of the tertiary
23
24 aerosols, passed through the spray chamber. The D_{50} values of the tertiary aerosols
25
26 obtained with the CGrid were smaller than those with the OneNeb in the range of the
27
28 liquid flow rate of 0.25 mL min⁻¹ to 2.0 mL min⁻¹ (2.8 μm to 3.1 μm for CGrid and 3.2
29
30 μm to 3.7 μm for OneNeb).
31
32
33
34

35
36 The ratio of the sensitivity obtained with the CGrid to those obtained with the other
37
38 nebulizers for the set of the emission lines listed in Table 2 was shown in Fig. 7, where
39
40 the liquid flow rates were set at 1 mL min⁻¹ for the CGrid, and 2.0 mL min⁻¹ for MHN,
41
42 m-HPCN, for obtaining the maximum sensitivities for each nebulizer. It is clearly seen
43
44 that the sensitivities obtained with the CGrid for all the measured lines were 1.2- to
45
46 3.5-fold higher than those with the other nebulizers, as is similar to the trend seen in Fig.
47
48 6. In comparison with MHN, the sensitivity obtained with the CGrid showed better
49
50 performance with high in energy sum (E_{sum}) value, while this trend was not observed in
51
52 comparison with m-HPCN and OneNeb. This difference was most likely due to the
53
54 difference in the plasma robustness obtained with each nebulizer. The robustness
55
56
57
58
59
60

1
2
3
4 index value of the plasma (Mg(II) 280.269 nm/Mg(I) 285.213 nm) by using the CGrid
5
6 (10.6) was almost the same as m-HPCN (10.2) and OneNeb (10.4) and much better than
7
8 that for MHN (9.2). When suitable plasma operating conditions are set, water vapor
9
10 can play a beneficial role in improving plasma characteristics such as electron density
11
12 through the release of hydrogen, which is the molecular gas with the highest thermal
13
14 conductivity under plasma conditions.⁴⁰⁻⁴³ In the case of the CGrid, the amount of
15
16 water vapor loading into the plasma was likely larger than the other nebulizers due to its
17
18 finer primary aerosols, which allowed easier evaporation in the spray chamber, thereby
19
20 improving the plasma robustness. The precision of measurements obtained with the
21
22 CGrid were similar to those obtained with the other nebulizer for all emission lines
23
24 tested. Relative standard deviation (RSD) values range between 0.3 % and 3.2 % for
25
26 the CGrid and between 0.5 % and 5.0 % for MHN, 0.3 % and 3.7 % for m-HPCN, and
27
28 0.3 % and 3.0 % for OneNeb. Consequently, the CGrid provided the higher sensitivity
29
30 in ICP-OES, corresponding to higher loading amount of fine aerosols into the plasma.
31
32
33
34
35
36

37 *Limit of detection (LOD)*

38
39 The LOD in ICP-OES obtained with the CGrid and the other nebulizers for the set
40
41 of the lines are summarized in Table 5, where the liquid flow rates were set at 1.0 mL
42
43 min⁻¹ for the CGrid and OneNeb, and 2.0 mL min⁻¹ for MHN and m-HPCN, for
44
45 obtaining the maximum sensitivities for each nebulizer. The CGrid provided lower
46
47 LODs than MHN for all the emission lines evaluated, except for Cd I 228.802 nm,
48
49 reflecting the sensitivity. The LOD for Cd I 228.802 nm was slightly worse than that
50
51 obtained with MHN. On the other hand, the LODs obtained with m-HPCN and
52
53 OneNeb were almost the same as those with the CGrid, though the CGrid provided
54
55
56
57
58
59
60

1
2
3
4 better sensitivities than m-HPCN. This would be owing to increase in the spectral
5
6 background originated from the solvent loading into the plasma. The increase of the
7
8 spectral background would compensate higher sensitivity. The CGrid provides higher
9
10 solvent loading amount than m-HPCN, as is seen in Fig.4.
11

12 13 14 15 *Memory effect*

16
17 A wash-in and wash-out performance in ICP-OES was checked for evaluating the
18
19 memory effect. No serious memory effect caused by the CGrid was observed, on
20
21 comparing the other nebulizers. The wash-in and wash-out times obtained with the
22
23 CGrid were around 15 second and 45 second, respectively, and were almost the same as
24
25 those with the other nebulizers. In the case of the Hildebrand nebulizer, which has the
26
27 two grid inside the nozzle, has the potential of a large memory effect, because sample
28
29 solution can easily be caught in the space between the grids.³⁰ On the contrary, in the
30
31 case of the CGrid, the premixing space inside the nozzle is adequately small, and the
32
33 thickness of the grid screen is a thin. These structural features should prevent the
34
35 memory effect.
36
37
38
39
40
41

42 *Short-term stability and spike recovery test*

43
44 Short-term stability test and spike recovery test for seawater sample was
45
46 performed for the CGrid. The spiked seawater was continuously nebulized at a liquid
47
48 flow rate of 1.0 mL min⁻¹ with a nebulizer gas flow rate of 0.55 L min⁻¹ for 45 minutes
49
50 (3 minutes measurements x 15 times), and the recovery value for spiked elements was
51
52 calculated.
53

54
55 Good measurement stability was obtained; the relative standard deviation of
56
57
58
59
60

1
2
3
4 15-times measurement was within 3 % for all the emission lines evaluated. No trend
5
6 of increase and decrease in signal intensity was observed during 45 minutes, and the
7
8 variance range was 99 % to 106 % for all the emission lines evaluated. The recovery
9
10 values are summarized in Table 6. All the recovery values obtained with the CGrid
11
12 were in acceptable range (100 % to 102 %) and in good agreement with those with
13
14 m-HPCN and OneNeb. These results indicate that the CGrid can be adopted for an
15
16 analysis of a high salt containing sample such as seawater.
17
18
19
20

21 *Application to analysis of brown rice flour CRM*

22
23
24 Multielement analysis of NMIJ CRM 7532-a brown rice flour was performed to
25
26 assess the reliability of analysis using the CGrid. The analytical results obtained with
27
28 the CGrid and MHN are summarized in Table 7. Although both analytical results were
29
30 in good agreement with the certified values, the precision of the results obtained with
31
32 the CGrid were superior to those obtained the MHN. The relative standard deviations
33
34 of the results obtained with the CGrid were in the range of 0.7 % for Mn to 3.2 % for Cd,
35
36 and were better than those obtained with the MHN (1.5 % for Mm to 6.9 % for Cd).
37
38 These results indicate that the CGrid can perform reliable ICP-OES measurements. In
39
40 comparison to conventional sample introduction systems, the CGrid has achieved a
41
42 drastic downsizing of sample consumption without sacrificing accuracy and precision.
43
44
45
46
47

48 **CONCLUSION**

49
50
51
52
53 A novel concentric type grid nebulizer (CGrid) was developed for ICP-OES.
54
55 Both on a nebulization efficiency and TDS tolerance, the CGrid was superior to MHN
56
57
58
59
60

1
2
3
4 and m-HPCN, and comparable with OneNeb. The CGrid can generate fine aerosols,
5
6 and the velocity is lower than the other nebulizers, resulting in a high sensitivity and
7
8 robustness in ICP-OES. The sensitivity obtained with the CGrid was 1.2- to 4.5-fold
9
10 higher than those with the other nebulizers. Although a larger amount of aerosol was
11
12 loaded into the plasma when using the CGrid, the plasma robustness indexed with the
13
14 ratio Mg(II)/Mg(I) was the same or slightly better than those obtained with the other
15
16 nebulizers. Saturated NaCl solution could be continuously nebulized for 5 hours,
17
18 without any washing. No serious memory effect caused by the CGrid was observed,
19
20 and acceptable analytical performances were shown in the analysis of seawater and rice
21
22 flour samples. We concluded that the new CGrid nebulizer described here is a very
23
24 useful nebulizer for ICP-OES with good performance.
25
26
27
28
29

30 ACKNOWLEDGEMENT

31
32
33
34
35 The authors express sincere appreciation to S.T. Japan inc. and Mr. Masaaki Abe
36
37 for supporting the present research. This work was partly supported by Grant-in-Aid
38
39 for Scientific Research (C) (No. 24550112) from the Japan Society for the Promotion of
40
41 Science.
42
43
44
45

46 REFERENCES

- 47
48
49
50
51 1. J. Nölte, *ICP Emission Spectrometry: A Practical Guide*, Wiley-VCH, Weinheim,
52
53 2003.
54
55 2. A. Montaser, D. W. Golightly, *Inductively Coupled Plasmas in Analytical Atomic*
56
57
58
59
60

- 1
2
3
4 *Spectrometry*, Wiley-VCH, Weinheim, 1992.
- 5
6 3. J. L. Todolí and J. M. Mermet, *Liquid Sample Introduction in ICP Spectrometry: A*
7
8 *Practical Guide*, Elsevier, 2008.
- 9
10 4. J. W. Olesik and J. C. Fister III, *Spectrochim. Acta, Part B*, 1991, **46**, 851-868.
- 11
12 5. S. E. Hobbs and J. W. Olesik, *Anal. Chem.*, 1992, **64**, 274-283.
- 13
14 6. J. W. Olesik and L. C. Bates, *Spectrochim. Acta, Part B*, 1995, **50**, 285-303.
- 15
16 7. M. P. Dziewatkoski, L. B. Daniels and J. W. Olesik, *Anal. Chem.*, 1996, **68**,
17
18 1101-1109.
- 19
20 8. O. Butler, W. Cairns, J. Cook and C. Davidson, *J. Anal. At. Spectrom.*, 2013, **28**,
21
22 177-216.
- 23
24 9. 4. E. Evans, M. Horstwood, J. Pisonero and C. Smith, *J. Anal. At. Spectrom.*, 2013,
25
26 **28**, 779-800.
- 27
28 10. P. Pohl and J. Dedina, *J. Anal. At. Spectrom.*, 2013, **28**, 175-176.
- 29
30 11. A. Taylor, M. Day, S. Hill, J. Marshall, M. Patriarca and M. White, *J. Anal. At.*
31
32 *Spectrom.*, 2013, **28**, 425-459.
- 33
34 12. S. Carter, A. Fisher, M. Hinds and S. Lancaster, *J. Anal. At. Spectrom.*, 2012, **27**,
35
36 2003-2053.
- 37
38 13. A. M. Gañán-Calvo, *Phys. Rev. Lett.*, 1998, **80**, 285-288.
- 39
40 14. A. M. Gañán-Calvo, *Appl. Phys. Lett.*, 2005, **86**, 214101.
- 41
42 15. J. Rosell-Llompart, A. M. Gañán-Calvo, *Phys. Rev. E*, 2008, **77**, 036321.
- 43
44 16. B. Almagro, A. M. Gañán-Calvo, A. Canals, *J. Anal. At. Spectrom.*, 2004, **19**,
45
46 1340-1346.
- 47
48 17. S. Groom, G. Schaldach, M. Ulmer, P. Walzel, H. Berndt, *J. Anal. At. Spectrom.*,
49
50 2005, **20**, 169-175.
- 51
52
53
54
55
56
57
58
59
60

- 1
2
3
4 18. B. Almagro, A.M. Gañan-Calvo, M. Hidalgo, A. Canals, *J. Anal. At. Spectrom.*,
5 2006, **21**, 770-777.
6
7
8
9 19. B. Almagro, A.M. Gañan-Calvo, M. Hidalgo, A. Canals, *J. Anal. At. Spectrom.*,
10 2006, **21**, 1072-1075.
11
12 20. H. Matusiewicz, M. Ślachciński, M. Hidalgo; A. Canals, *J. Anal. At. Spectrom.*,
13 2007, **22**, 1174-1178.
14
15
16
17 21. H. Matusiewicz, M. Ślachciński, B. Almagro, A. Canals, *Chem. Anal. (Warsaw)*,
18 2009, **54**, 1219-1244.
19
20
21 22. M A. Aguirre, N. Kovachev, B. Almagro, M. Hidalgo, A. Canals, *J. Anal. At.*
22 *Spectrom.*, 2010, **25**, 1724-1732.
23
24
25 23. G.L. Donati, R.S. Amais, D. Schiavo, J.A. Nóbrega, *J. Anal. At. Spectrom.*, 2013,
26 **28**, 755-759.
27
28
29 24. R.S. Amais, G.L. Donati, D. Schiavo, J.A. Nóbrega, *Microchem. J.*, 2013, **106**,
30 318-322.
31
32
33 25. K.Inagaki, S. Fujii, A. Takatsu, K. Chiba, *J. Anal. At. Spectrom.*, 2011, **26**, 623-630.
34
35
36 26. Y. Takasaki, S. Sakagawa, K. Inagaki, S. Fujii, A. Sabarudin, T. Umemura, H.
37 Haraguchi, *Anal. Chim. Acta*, 2012, **713**, 23-29.
38
39
40 27. Y. Takasaki, K. Inagaki, A. Sabarudin, S. Fujii, D. Iwahata, A. Takatsu, K. Chiba, T.
41 Umemura, *Talanta*, 2011, **87**, 24-29.
42
43
44 28. A. S. Groombridge, K. Inagaki, S. Fujii, K. Nagasawa, T. Okahashi, A. Takatsu, and
45 K. Chiba, *J. Anal. At. Spectrom.*, 2012, **27**, 1787-1793.
46
47
48 29. T. Brotherton, B. Barnes, N. Vela and J. Caruso, *J. Anal. At. Spectrom.*, 1987, **2**,
49 389-396.
50
51
52 30. T. Brotherton and J. Caruso, *J. Anal. At. Spectrom.*, 1987, **2**, 695-698.
53
54
55
56
57
58
59
60

- 1
2
3
4 31. S. HighT and J. Rader, *Analyst*, 1991, **2**, 389-396.
5
6 32. H. Matusiewicz, *J. Anal. At. Spectrom.*, 1993, **8**, 961-964.
7
8 33. J. M. Mermet, *Spectrochim. Acta Part B*, 1989, **44**, 1109-1116.
9
10 34. K. W. Olson, W. J. Haas, V. A. Fassel, *Anal. Chem.*, 1977, **49**, 632-637.
11
12 35. D. D. Smith, R. F. Browner, *Anal. Chem.*, 1982, **54**, 533-537.
13
14 36. A. Gustavsson, *Spectrochim. Acta, Part B*, 1984, **39**, 743-746.
15
16 37. H. E. Pace, N. j. Rogers, C. Jarolimek, V. A. Coleman, C. P. Higgins, J. F. Ranville,
17
18 *Anal. Chem.*, 2011, **83**, 9361-9369.
19
20 38. E. Paredes, J. Bosque, J. M. Mermet, J. L. Todolí, *Spectrochim. Acta Part B*, 2010
21
22 **65**, 908-917.
23
24 39. K. Kahen, K. Jorabchi, C. Gray, A. Montaser, *Anal. Chem.*, 2004, **76**, 7194-7201.
25
26 40. I. Novotny, J. C. Farinas, W. Jia-liang, E. Poussel, J. M. Mermet, *Spectrochim. Acta*
27
28 *Part B*, 1996, **51**, 1517-1526.
29
30 41. M. Grotti, C. Lagomarsino, J. M. Mermet, *J. Anal. At. Spectrom.*, 2006, **21**,
31
32 963-969.
33
34 42. S.E.Long, R. F. Browner, *Spectrochim. Acta Part B*, 1986, **41**, 639-649.
35
36 43. S.E.Long, R. F. Browner, *Spectrochim. Acta Part B*, 1988, **43**, 1461-1471.
37
38
39
40
41
42
43
44
45
46
47
48
49
50
51
52
53
54
55
56
57
58
59
60

Table 1 Operating conditions of the ICP-OES.

Incident Rf power	1.4 kW
Frequency	40 MHz
Outer gas flow rate	15 L min ⁻¹
Intermediate gas flow rate	0.2 L min ⁻¹
Sheath gas	Nitrogen 0.3 L min ⁻¹
Torch injector	Alumina (i.d. 1 mm)
Spray chamber	Twister cyclone chamber (baffled)
Nebulizer gas flow rate	0.55 L min ⁻¹ - 0.58 L min ⁻¹ for CGrid, OneNeb 0.60 L min ⁻¹ - 0.63 L min ⁻¹ for MHN, m-HPCN
Liquid nebulizer gas flow rate	0.25 mL min ⁻¹ - 2.0 mL min ⁻¹
Integration time	0.5 s-10.0 s (automatically)
Read time	1 s
Measurement repeats	5 times
View mode	Axial

Table 2 Energy values for the emission lines.

Emission type	Element	Wavelength / nm	E_{ion} / eV	E_{exc} / eV	E_{sum} / eV
Atomic line	Cr I	357.87		3.5	3.5
	Cu I	327.39		3.8	3.8
	Mg I	285.21		4.4	4.4
	Mn I	279.48		4.4	4.4
	Ni I	232.00		5.4	5.4
	Cd I	228.80		5.4	5.4
	Pb I	217.00		5.7	5.7
	Zn I	213.86		5.8	5.8
Ionic line	Cr II	267.72	6.8	4.6	11.4
	Mg II	280.27	7.7	4.5	12.1
	Mn II	257.61	7.9	4.4	12.3
	Ni II	231.60	7.6	5.4	13.0
	Pb II	220.35	7.4	5.6	13.0
	Fe II	238.20	7.9	5.2	13.1
	Cu II	224.70	7.7	5.6	13.3
	Cd II	214.44	9.0	5.8	14.8
Zn II	206.20	9.4	6.0	15.4	

Table 3 Summary of the D_{50} and D_{90} values of the primary aerosols at the liquid flow rate of 1.0 mL min^{-1} with the nebulizer gas flow rate of 1.0 L min^{-1} and optimized gas flow rates.¹

	Nebulizer gas flow rate		Nebulizer gas flow rate	
	1.0 L min^{-1}		Optimized ¹	
	D_{50} / mm	D_{90} / mm	D_{50} / mm	D_{90} / mm
CGrid	3.1	10.7	4.0	10.3
MHN	14.9	41.7	25.8	53.8
m-HPCN	3.4	10.7	5.8	12.5
OneNeb	3.4	11.1	5.9	12.3

¹Optimized to obtain the highest value of the ratio Mg(II) 280.269 nm/Mg(I) 285.213 nm: 0.55 L min^{-1} for CGrid and OneNeb, 0.60 L min^{-1} for MHN and m-HPCN.

Table 4 Summary of transport efficiencies of aerosols into the plasma in the range of a liquid flow rate of 0.25 mL min^{-1} to 2.0 mL min^{-1} .

Liquid flow rate (mL min^{-1})	CGrid TE (%) ¹	MHN TE (%) ¹	m-HPCN TE (%) ¹	OneNeb TE (%) ¹
0.25	81.5 ± 1.4	22.3 ± 0.7	53.3 ± 0.9	63.1 ± 1.1
0.50	49.7 ± 0.8	16.7 ± 0.5	31.3 ± 0.5	42.1 ± 0.7
0.75	35.2 ± 0.6	15.0 ± 0.4	23.2 ± 0.4	34.1 ± 0.5
1.00	27.9 ± 0.5	11.1 ± 0.3	18.0 ± 0.3	25.9 ± 0.4
1.50	18.6 ± 0.3	8.4 ± 0.3	13.6 ± 0.2	18.2 ± 0.3
2.00	14.1 ± 0.2	6.6 ± 0.2	10.4 ± 0.2	13.8 ± 0.2

¹TE: transport efficiency (average \pm standard uncertainty, $n = 3$), which was calculated from the loading amount of aerosols.

Table 5 Analytical detection limit obtained with CGrid and the other nebulizers.

Element	Wavelength / nm	CGrid / $\mu\text{g kg}^{-1}$	MHN / $\mu\text{g kg}^{-1}$	OneNeb / $\mu\text{g kg}^{-1}$	m-HPCN / $\mu\text{g kg}^{-1}$
Cr I	357.87	1.9	7	2.0	3
Cu I	327.39	3	6	4	2
Mg I	285.21	0.9	1.8	0.4	0.8
Mn I	279.48	4	7	5	5
Ni I	232.00	1.3	3	0.9	1.6
Cd I	228.80	0.4	0.3	0.18	0.20
Pb I	217.00	10	30	9	6
Zn I	213.86	0.3	0.7	0.23	0.15
Cr II	267.72	0.14	0.7	0.4	0.4
Mg II	280.27	0.07	0.23	0.18	0.3
Mn II	257.61	0.03	0.07	0.03	0.05
Ni II	231.60	0.6	1.6	0.5	0.6
Pb II	220.35	1.6	6	1.3	2.1
Fe II	238.20	0.3	0.7	0.18	0.18
Cu II	224.70	3	6	5	1.6
Cd II	214.44	0.20	0.4	0.09	0.16
Zn II	206.20	0.19	1.0	0.4	0.3

Table 6 Recovery values of spiked seawater CRM at the liquid flow rate of 1 mL min^{-1} .

Element	Wavelength / nm	CGrid recovery (%) ¹ (n = 3)	m-HPCN recovery (%) ¹ (n = 3)	OneNeb recovery (%) ¹ (n = 3)
Cr	267.72	100.5 ± 1.3	101.3 ± 1.4	101.0 ± 1.3
Mn	257.61	100.8 ± 1.5	102.6 ± 2.0	102.1 ± 2.1
Fe	238.20	100.6 ± 1.9	102.6 ± 2.4	102.0 ± 2.4
Ni	231.60	101.4 ± 3.0	103.3 ± 2.7	102.7 ± 2.7
Cu	224.70	100.3 ± 1.9	99.0 ± 3.4	99.2 ± 3.0
Zn	206.20	101.5 ± 4.9	105.5 ± 5.5	104.4 ± 5.3
Cd	214.44	100.6 ± 3.4	104.0 ± 4.5	103.2 ± 4.3
Pb	220.35	101.8 ± 3.8	103.7 ± 3.1	103.0 ± 3.2

¹ Spiked level: 0.5 mg kg^{-1} in the solution. The intensity was corrected by the internal standard method, where Y (0.5 mg kg^{-1}) was used as the internal standard.

Table 7 Analytical results for NMIJ CRM 7531-a white rice flour obtained by ICP-OES with the CGrid and MHN.

Element	Observed value ¹	Observed value ¹	Certified value ²
	obtained with CGrid	obtained with MHN	
	mg kg ⁻¹	mg kg ⁻¹	mg kg ⁻¹
Mn	27.7 ± 0.2	27.2 ± 0.4	27.6 ± 0.7
Fe	11.8 ± 0.2	12.0 ± 0.2	11.66 ± 0.32
Cu	4.40 ± 0.05	4.43 ± 0.09	4.34 ± 0.13
Zn	31.8 ± 0.3	29.7 ± 0.5	31.8 ± 0.7
Cd	0.31 ± 0.01	0.29 ± 0.02	0.308 ± 0.007

¹ Mean ± standard deviation ($n = 3$)

² Property value ± expanded uncertainty (coverage factor $k = 2$)

FIGURE CAPTIONS

Fig. 1 Schematic image of the CGrid.

Fig. 2 Comparison of the primary droplet diameter distributions by using the CGrid, MHN, m-HPCN, and OneNeb: liquid flow rate $Q_l = 1.0 \text{ mL min}^{-1}$; gas flow rate $Q_g = 0.55 \text{ L min}^{-1}$ for CGrid and OneNeb, 0.60 L min^{-1} for MHN and m-HPCN.

Fig. 3 Two dimensional distribution map of droplet diameter and velocity of primary aerosols generated with (a) CGrid, (b) MHN, (c) m-HPCN, and (d) OneNeb. $Q_l = 1.0 \text{ mL min}^{-1}$, $Q_g = 0.6 \text{ L min}^{-1}$.

Fig. 4 Relative volume amount of aerosols loading into the plasma by using the CGrid, MHN, m-HPCN, and OneNeb: $Q_l = 0.25 \text{ mL min}^{-1}$ to 2.0 mL min^{-1} , $Q_g = 0.55 \text{ L min}^{-1}$ to 0.58 L min^{-1} for CGrid and OneNeb, 0.60 L min^{-1} to 0.63 L min^{-1} for MHN and m-HPCN.

Fig. 5 Photo image of the grid screen (a) before and (b) after nebulizing of saturated NaCl solution.

Fig. 6 Relative signal intensities of Mn(II) 257.610 nm in ICP-OES obtained with the CGrid, MHN, m-HPCN, and OneNeb: $Q_l = 0.25 \text{ mL min}^{-1}$ to 2.0 mL min^{-1} , $Q_g = 0.55 \text{ L min}^{-1}$ to 0.58 L min^{-1} for CGrid and OneNeb, 0.60 L min^{-1} to 0.63 L min^{-1} for MHN and m-HPCN. Measured solution : 0.5 mg kg^{-1} of Mn standard solution.

1
2
3
4
5
6
7
8
9
10
11 **Fig. 7** Comparison of the sensitivity in ICP-OES obtained with the CGrid and those
12 with MHN, m-HPCN, and OneNeb.
13

14
15 CGrid : $Q_g = 0.55 \text{ L min}^{-1}$; $Q_l = 1.0 \text{ mL min}^{-1}$, MHN and m-HPCN: $Q_g = 0.63 \text{ L min}^{-1}$;

16
17 $Q_l = 2.0 \text{ mL min}^{-1}$, OneNeb: $Q_g = 0.58 \text{ L min}^{-1}$; $Q_l = 1.0 \text{ mL min}^{-1}$.

18
19 Measured solution : 0.5 mg kg^{-1} of multielement standard solution.
20
21
22
23
24
25
26
27
28
29
30
31
32
33
34
35
36
37
38
39
40
41
42
43
44
45
46
47
48
49
50
51
52
53
54
55
56
57
58
59
60

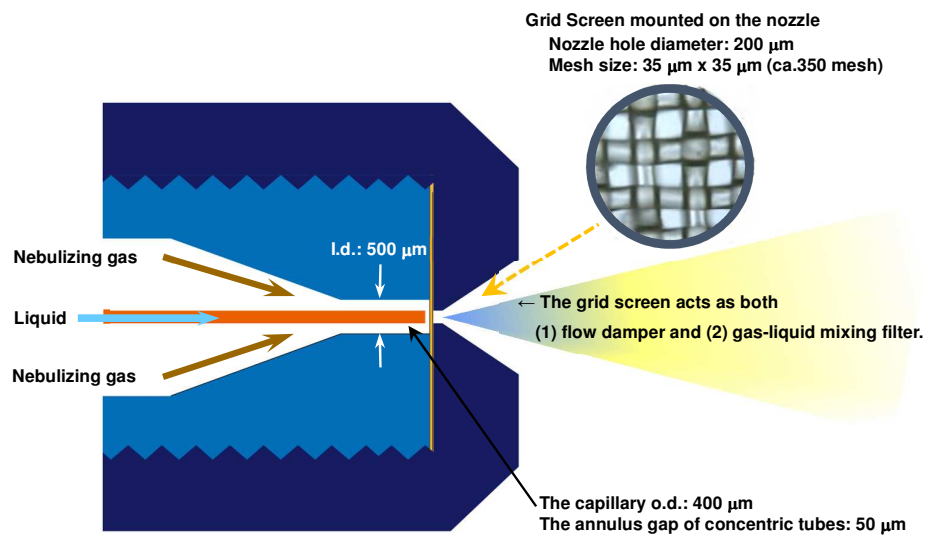


Fig. 1 K. Inagaki et al.

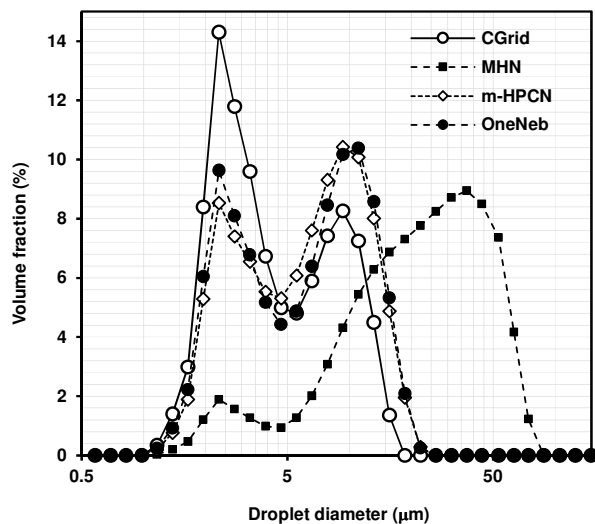
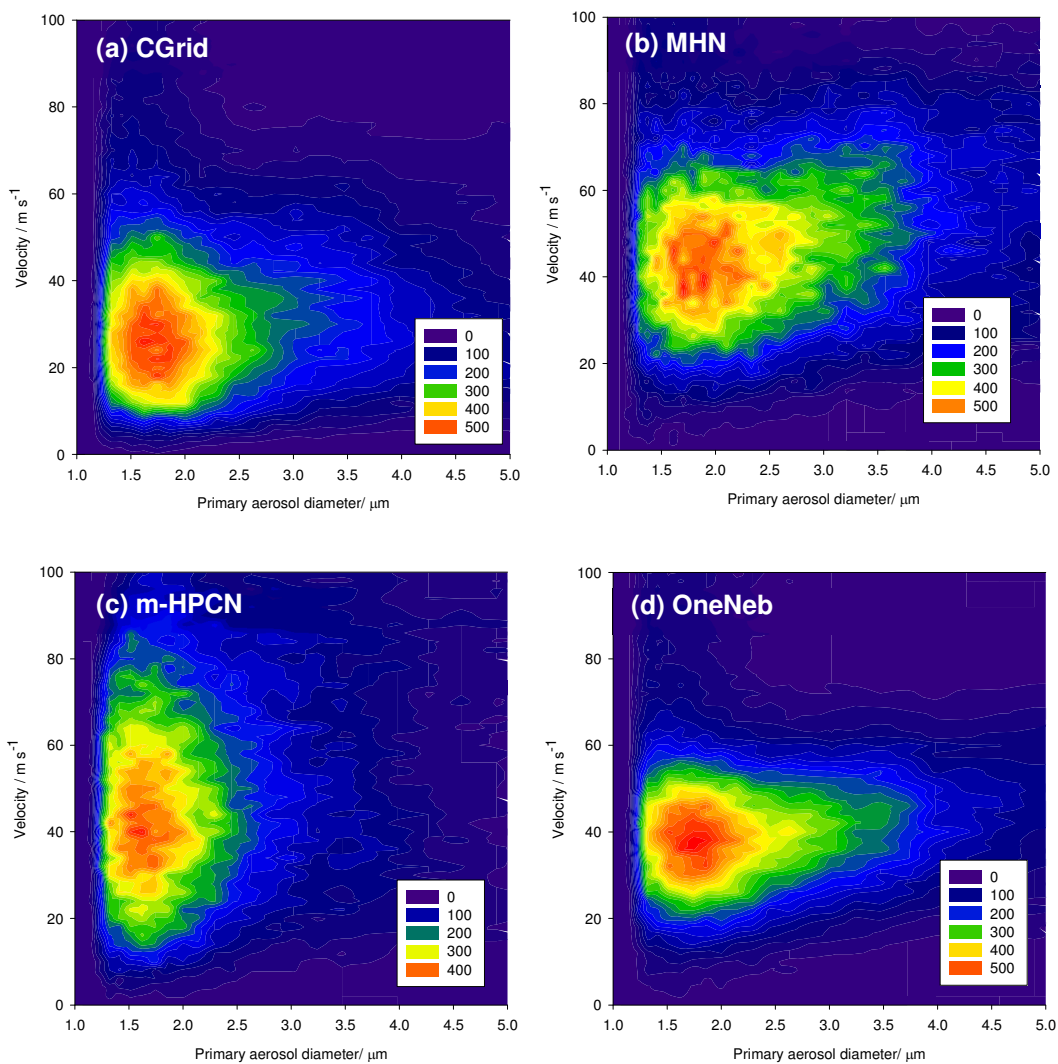


Fig. 2 K. Inagaki et al.



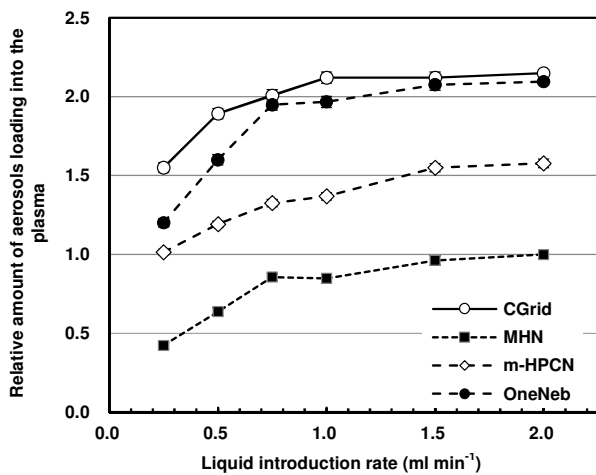


Fig. 4 K. Inagaki et. al.

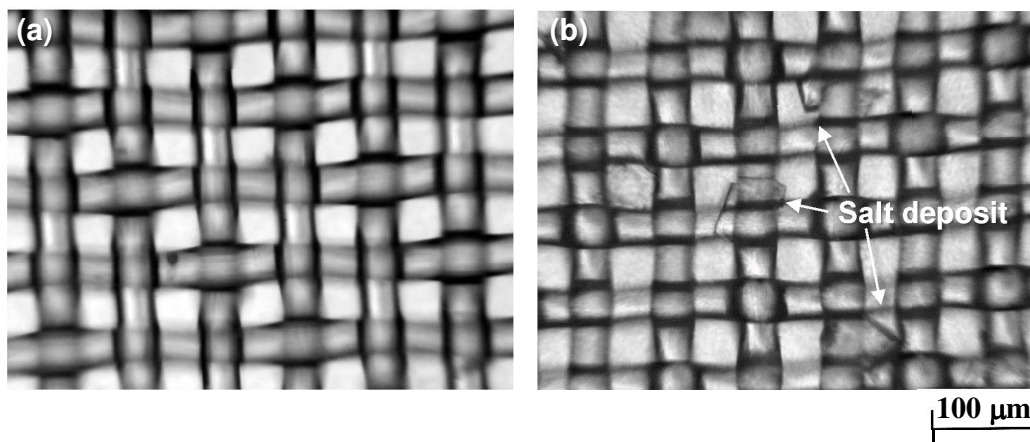


Fig. 5 K. Inagaki et. al.

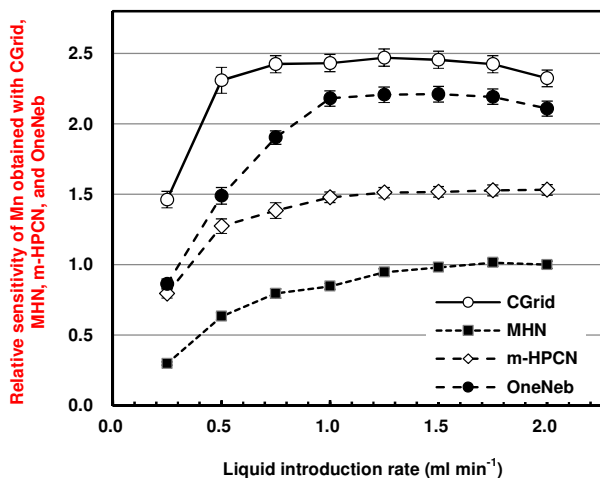


Fig. 6 K. Inagaki et. al.

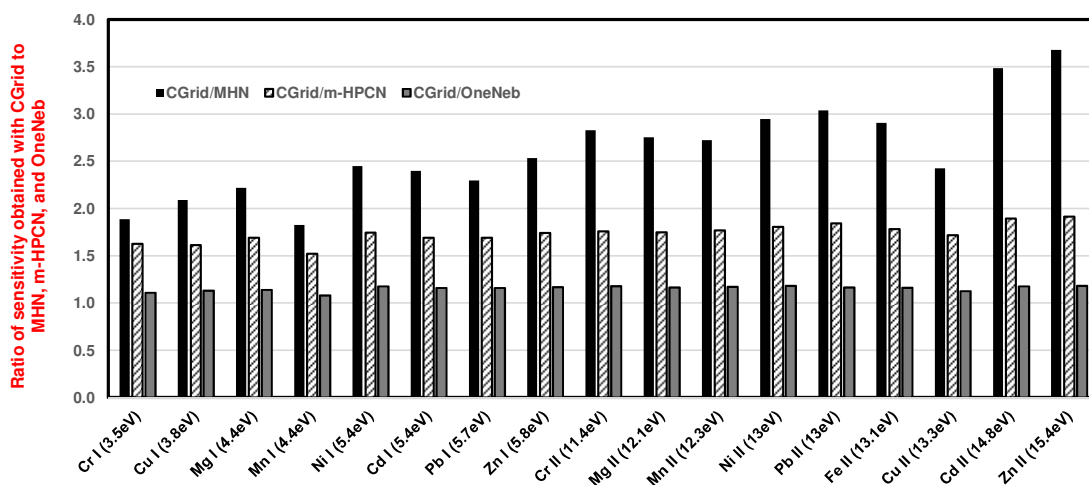


Fig. 7 K. Inagaki et. al.